Optimizing Formation Rigidity Under Connectivity Constraints

Yanghyun Kim, Guangwei Zhu and Jianghai Hu

***Abstract*— This paper studies the problem of finding the most rigid formation for a multi-agent system. The worst-case rigidity index (WRI) and the mean rigidity index (MRI) are proposed as the quantitative measures of formation rigidity. From a practical point of view, the values of these indices characterize the stability and robustness of the multi-agent system in maintaining a given formation. An iterative algorithm is presented for finding the most rigid formation through the joint optimization of both the positions of agents and their connection topology. The effectiveness of the algorithm is illustrated through numerical examples.**

***Index Terms*— formation control, graph rigidity, wireless sensor network, optimization**

I. Introduction

Tasks arising in many practical applications such as aerospace, battle field and emergency services, are often difficult or even impossible for a single agent (vehicle, aircraft, etc.) to accomplish as a large region with much uncertainty needs to be covered/monitored. Completing these tasks may become feasible through the coordination of a group of autonomous agents. For maximal coordination efficiency, it is often advantageous for these agents to maintain a certain formation through sensing and communications. The formation control of multi-agent systems has been studied by many researchers in various contexts, such as robotics, unmanned air vehicle (UAV) [1], underwater vehicles [2] and so on [3], [4].

Rigidity is a critical concept in the study of formation control as it characterizes the ability of a multi-agent system to maintain a desired formation despite the presence of (possibly significant) sensing errors, communication delays, and environmental perturbations. An early paper on applying the notion of rigidity to multi-agent systems can be found in [5], which employed results in graph theory such as the Laman's theorem [6] and the rigidity matrix theorem [7], [8] to determine *qualitatively* whether a formation is rigid or non-rigid. Dynamics of formation such as splitting, merging [3], and closing ranks [9] have also been explored.

In [10], *quantitative measures* of formation rigidity are proposed based on the notion of stiffness matrix by analogizing a formation to a mass-spring system: each node (agent) corresponds to a mass and each edge (communication link) connecting a pair of nodes corresponds to a spring with a given elastic constant. The rigidity indices are then derived from the eigenvalues of the stiffness matrix associated with the overall elastic structure. With these quantitative measures, one can now formally compare the degree of rigidity among different formations previously only known to be rigid.

In this paper, we focus on two quantitative measures of formation rigidity: the worst rigidity index (WRI) first proposed in [10] and a novel measure called the mean rigidity index (MRI). Furthermore, we try to find the most rigid formations as measured by these indices through an iterative algorithm that optimizes both the node locations and the formation topology simultaneously. Such optimized formations typically result in better robustness of the multi-agent systems on formation control or localization tasks.

This paper is organized as follows. The two rigidity indices derived from the stiffness matrix are discussed in Section II. The formation rigidity optimization problem is formulated in Section III. Section IV discusses the optimization of agent position. In Section V, the edge-by-edge topology switching algorithm is introduced as the topology optimization method. Section VI illustrates an alternative algorithm that simultaneously optimizes the discrete topology and the continuous agent positions. Some examples are shown in Section VII. Section VIII summarizes the paper.

A. Notation

Throughout this paper, $\mathbb{R}, \mathbb{R}^n, \mathbb{R}^{n\times m}$ denote the spaces of real numbers, n-dimensional real column vectors, and n-by-m real matrices, respectively. Italic lowercase letters, with or without subscripts, e.g., k_{ij}, r, represent scalar variables or constants. Italic uppercase letters, such as R, K, S_{ij}, are matrices. Calligraphic letters, e.g., $\mathcal{I}, \mathcal{C}$, denote general sets. Column vectors are denoted by bold letters. The transpose of $\mathbf{v} \in \mathbb{R}^n$ (or $A \in \mathbb{R}^{n\times m}$) is denoted by $\mathbf{v}^\top$ (or $A^\top$). A vector is called a *multi-quantity* if it is a stacked vector composed by several quantities which themselves are vectors. A bold lowercase letter with no subscript often denotes a multi-quantity, and each of its components is denoted by the same letter with a subscript. For example, $\mathbf{p} \in \mathbb{R}^{2n}$ is a *multi-point*, $\mathbf{p} = \begin{bmatrix}\mathbf{p}_1^\top & \mathbf{p}_2^\top & \cdots & \mathbf{p}_n^\top\end{bmatrix}^\top$; each component $\mathbf{p}_i \in \mathbb{R}^2$ represents the two-dimensional coordinate of a point in an n-point system. The inner product of two vectors $\mathbf{u}, \mathbf{v} \in \mathbb{R}^n$ is defined as $\langle \mathbf{u}, \mathbf{v}\rangle = \mathbf{u}^\top\mathbf{v} \in \mathbb{R}$. The Euclidean norm of a vector $\mathbf{v}$ is denoted by $\|\mathbf{v}\| = \sqrt{\langle \mathbf{v}, \mathbf{v}\rangle}$. For symmetric matrices A, B, we write $A \succeq 0$ if A is non-negative definite; $A \succeq B$ if $A - B \succeq 0$. The Moore-Penrose pseudo-inverse of a square matrix $A \in \mathbb{R}^{n\times n}$ is denoted by $A^\dagger$. Let $G = (\mathcal{V}, \mathcal{E})$ be a graph with a set of vertices $\mathcal{V}$ and a set of edges $\mathcal{E}$. Then $\mathcal{E}^\complement$ denotes the set of all missing edges (i.e., edges not in $\mathcal{E}$).

Yanghyun Kim, Guangwei Zhu, and Jianghai Hu are with the School of Electrical and Computer Engineering, Purdue University, West Lafayette, IN 47907, USA {yhkim,guangwei,jianghai}@purdue.edu.

II. Background

In this section, derivation of the rigidity indices to be used in this paper is reviewed. Suppose there are n agents moving in a two-dimensional space $\mathbb{R}^2$, whose locations are denoted by $\mathbf{p}_i \in \mathbb{R}^2$, $i \in \mathcal{I} = \{1, \dots, n\}$. The strength of the communication link (or the sensing data correlation) between each pair of agents i and j is modeled by a scalar constant $k_{ij} \geq 0$. We assume that $k_{ij} = k_{ji}$; and that $k_{ij} = 0$ if agents i and j do not communicate with each other directly. Particularly, let $k_{ij} = 0$ when $i = j$. Then the connectivity matrix is defined as $K = [k_{ij}]_{1 \leq i,j \leq n}$. In this formulation, the n agents form a weighted graph, with each node of the graph being an agent and edge weights represented by the entries of the connectivity matrix K. This graph with weights k_{ij} and node positions $\mathbf{p}_i$ specifies a *formation graph*, or simply, a KP-formation. A KP-formation is described by a tuple $(\mathcal{I}, \mathbf{p}, K)$ in this paper.

A. Stiffness Matrix

To study the robustness of a KP-formation under perturbations, a mechanical analogy is constructed as follows. Each node (agent) is modeled by a mass, and the edge connecting nodes i and j is modeled by a spring with spring constant k_{ij} and natural length $\|\mathbf{p}_i - \mathbf{p}_j\|$. Thus, the springs are all relaxed for the original node positions $\mathbf{p}_1, \dots, \mathbf{p}_n$. Now assume the position of each node i is perturbed to $\hat{\mathbf{p}}_i = \mathbf{p}_i + \Delta\mathbf{p}_i \in \mathbb{R}^2$ after a net perturbation $\Delta\mathbf{p}_i$, $i = 1, \dots, n$. This results in a deviation of the length of the spring between two nodes i and j from its natural length. Denote by $\mathbf{f}_{ij} \in \mathbb{R}^2$ the resulting force applied on node i by node j. By the Hooke's law,

$$\|\mathbf{f}_{ij}\| = k_{ij} \big| \|\hat{\mathbf{p}}_i - \hat{\mathbf{p}}_j\| - \|\mathbf{p}_i - \mathbf{p}_j\| \big|. \tag{1}$$

Consider infinitesimally small perturbations $\Delta\mathbf{p}_i$, $i = 1, \dots, n$. Denote by $E_{ij} \in \mathbb{R}^{2\times 2}$ the projection matrix onto the direction of $\mathbf{p}_i - \mathbf{p}_j$:

$$E_{ij} = \frac{(\mathbf{p}_i - \mathbf{p}_j)(\mathbf{p}_i - \mathbf{p}_j)^\top}{\|\mathbf{p}_i - \mathbf{p}_j\|^2}. \tag{2}$$

Then $\Delta\mathbf{p}_i$ can be decomposed into an along-spring perturbation $E_{ij}\Delta\mathbf{p}_i$ and a cross-spring perturbation $(I_2 - E_{ij})\Delta\mathbf{p}_i$. For small perturbations, only the along-spring perturbations affect the spring length; thus, the infinitesimal change in spring length between nodes i and j is approximately

$$\big| \|\hat{\mathbf{p}}_i - \hat{\mathbf{p}}_j\| - \|\mathbf{p}_i - \mathbf{p}_j\| \big| \simeq \|E_{ij}\Delta\mathbf{p}_i - E_{ij}\Delta\mathbf{p}_j\|.$$

Hooke's equation is generalized to be

$$\mathbf{f}_{ij} = k_{ij}E_{ij}(\Delta\mathbf{p}_i - \Delta\mathbf{p}_j).$$

Let $\mathbf{f}_i = \sum_{j=1}^n \Delta\mathbf{f}_{ij}$ be the total force applied on node i, or

$$\mathbf{f}_i = \sum_{j \in \mathcal{I}} k_{ij}E_{ij}(\Delta\mathbf{p}_i - \Delta\mathbf{p}_j)$$

with the fact that $k_{ij} = 0$ if agents i and j are not neighbors. Denote $\mathbf{f} = [\mathbf{f}_1^\top \ \cdots \ \mathbf{f}_n^\top]^\top$, $\Delta\mathbf{p} = [\Delta\mathbf{p}_1^\top \ \cdots \ \Delta\mathbf{p}_n^\top]^\top \in \mathbb{R}^{2n}$. Then the above can be written in matrix form as

$$\mathbf{f} = -S\Delta\mathbf{p} \tag{3}$$

for a matrix $S = [S_{ij}]_{1 \leq i,j \leq n} \in \mathbb{R}^{2n\times 2n}$ where each block $S_{ij} \in \mathbb{R}^{2\times 2}$ is defined by

$$S_{ij} = \begin{cases} \sum_{j \in I} k_{ij}E_{ij} & \text{if } i = j \\ -k_{ij}E_{ij} & \text{if } i \neq j. \end{cases}$$

The matrix S is called the *stiffness matrix* associated with the KP-formation. We may write $S(K, \mathbf{p})$ to show its dependency on K and $\mathbf{p}$.

B. Rigidity Indices

According to (3), the stiffness matrix S describes the relation between the perturbation $\Delta\mathbf{p}$ in node positions and the resulting (resistance) force $\mathbf{f}$ that generally tries to return the formation to it original configuration. Intuitively, a more rigid formation should be one that the same amount of position perturbation $\Delta\mathbf{p}$ would result in a larger resistance force $\mathbf{f}$. More precisely, a rigidity index $r(S)$ is a scalar derived from the stiffness matrix S which measures the rigidity of a KP-formation. A valid rigidity index $r(S)$ should have the following properties:

Property 1. *Non-negativeness*: $r(S) \geq 0$ for any formation. Furthermore, $r(S) = 0$ if and only if the formation represented by S is not rigid.

Property 2. *Invariance*: $r(S)$ is invariant under rigid body motions and scaling of node positions of the formation.

Property 3. *Consistency*: $r(S)$ does not decrease when k_{ij} (connectivity) increases for any pair of nodes $i \neq j$.

These properties fit well our intuitive expectations of a measure of formation rigidity. Based on the above properties, two valid rigidity indices can be proposed:

$$r_{\mathrm{w}}(S) = \lambda_4(S),$$
$$\bar{r}(S) = \left(\sum_{k=4}^{2n} \frac{1}{\lambda_k(S)} \right)^{-1},$$

where $\lambda_k(S)$ is the k-th smallest eigenvalue of the matrix S. Particularly, $\bar{r}(S) := 0$ if $\lambda_4(S) = 0$. We call r_{w} the *Worst-case Rigidity Index (WRI)* and $\bar{r}$ the *Mean Rigidity Index (MRI)*. A proof of the validity of r_{w} as a rigidity index is given in [10]. This proof can also be applied to $\bar{r}$ after some minor changes.

We further note that, whenever a formation is rigid, the MRI can be rewritten in the following simpler form:

$$\bar{r}(S) = \big[\mathrm{tr}(S^\dagger)\big]^{-1}, \tag{4}$$

where $S^\dagger$ is the Moore-Penrose pseudo-inverse of S.

III. Formation Optimization Problem

In Section II, rigidity indices are obtained from the stiffness matrix which encodes information on both agent locations and formation topology. These indices can serve as quantitative measures of formation rigidity. A natural question that follows is: what are the most rigid formations as measured by these indices? The answer to this question will be useful in the design of more robust multi-agent systems.

A general KP-formation optimization problem based on a rigidity index $r(\cdot)$ can be formulated as follows:

$$\max_{K,\mathbf{p}} \quad r(S(K,\mathbf{p})). \tag{5}$$

With different choices of the rigidity index $r(\cdot)$, the objective function, hence the optimal solutions, will be different. Nonetheless, it can be expected that meaningful rigidity indices are all "comparable" because of the shared consistency property. In other words, a rigid formation measured by one index will tend to be also rigid in other indices. As a result, switching the rigidity index is not expected to affect the optimization results significantly.

In this paper, we pick the MRI as our objective function for the KP-formation optimization problem. An important practical implication of the MRI is its direct relation to the well-known Cramér-Rao lower bound (CRLB) in the network localization applications [11]. By optimizing the MRI, one can obtain a localization network formation with the lowest CRLB. This generally leads to a smaller total localization error in practice.

Without any constraint on the connectivity matrix K, the solution to problem (5) would be trivial as any rigidity index will increase to infinity as $K \to \infty$. In this paper, we consider the following constraint on K:

$$\text{subject to} \quad k_{ij} \in \{0,1\} \quad \text{and} \quad \sum_{i\in\mathcal{I}} \sum_{j\in\mathcal{I}\setminus i} k_{ij} = k_c,$$

where k_c is a constant integer equal to the total available communication channels in the formation. Under the above constraint, the optimization with respect to K is essentially a process of optimizing channel resource allocation, a useful problem in some practical applications.

To sum up, the KP-formation optimization problem to be solved in this paper is

$$\begin{aligned} \max_{K,\mathbf{p}} \quad & \bar{r}(S(K,\mathbf{p})) \\ \text{subject to} \quad & k_{ij} \in \{0,1\} \\ & \sum_{i\in\mathcal{I}} \sum_{j\in\mathcal{I}\setminus i} k_{ij} = k_c. \end{aligned} \tag{6}$$

Note that there is no constraint on $\mathbf{p}$, as the objective function is invariant under scaling and rigid body motions of $\mathbf{p}$. The optimal formation can be arbitrarily scaled, rotated and translated as one desires when applied to practical scenarios.

IV. Agent Positions Optimization

Solution of the optimization problem stated in (6) in Section III can be divided into two phases: optimizing agent positions $\mathbf{p}$ and optimizing formation topology K. In this section, optimization of agent positions will be discussed.

A. Problem Statement

In the agent positions optimization phase, one assumes that the connectivity matrix K is fixed and tries to find the agent positions $\mathbf{p}$ that results in the largest rigidity index, by solving the following problem:

$$\max_{\mathbf{p}} \quad \bar{r}(S(K,\mathbf{p})). \tag{7}$$

Here the MRI is chosen as the rigidity index in the objective function and K is assumed to be constant.

It is reasonable to assume that the initial formation from which the optimization starts is at least rigid, i.e., $\bar{r}(S_0) > 0$. Under this assumption, by recalling (4), the optimization problem (7) can be equivalently formulated as

$$\min_{\mathbf{p}} \quad \operatorname{tr}(S(K,\mathbf{p})^\dagger). \tag{8}$$

B. Gradient of Objective Function

Optimization problem (8) can be solved by computing the gradient of its objective function. We give a brief deduction of the gradient in this subsection. Some well-known facts in matrix calculus [12] are applied in the deduction.

Since both S and $S^\dagger$ are symmetric, we have

$$\mathrm{d}\,\operatorname{tr}(S^\dagger) = \operatorname{tr}(\mathrm{d}(S^\dagger)) = -\operatorname{tr}(S^\dagger S^\dagger \mathrm{d}S). \tag{9}$$

We define

$$X \triangleq S^\dagger S^\dagger = \begin{bmatrix} X_{11} & X_{12} & \cdots & X_{1n} \\ X_{21} & X_{22} & \cdots & X_{2n} \\ \vdots & \vdots & \ddots & \vdots \\ X_{n1} & X_{n2} & \cdots & X_{nn} \end{bmatrix}$$

where each X_{ij} is a 2-by-2 matrix, and $X_{ij} = X_{ji}^\top$ from the symmetry of X. On the other hand,

$$\mathrm{d}S = \begin{bmatrix} \sum\limits_{j\neq 1} k_{1j}\mathrm{d}E_{1j} & -k_{12}\mathrm{d}E_{12} & \cdots & -k_{1n}\mathrm{d}E_{1n} \\ -k_{21}\mathrm{d}E_{21} & \sum\limits_{j\neq 2} k_{2j}\mathrm{d}E_{2j} & \cdots & -k_{2n}\mathrm{d}E_{2n} \\ \vdots & \vdots & \ddots & \vdots \\ -k_{n1}\mathrm{d}E_{n1} & -k_{n2}\mathrm{d}E_{n2} & \cdots & \sum\limits_{j\neq n} k_{nj}\mathrm{d}E_{nj} \end{bmatrix} \tag{10}$$

with E_{ij} being the projection matrix defined in (2).

Suppose now we pick any $j \in \mathcal{I}$ and perturb only $\mathbf{p}_j$ while keeping $\mathbf{p}_i$'s constant for all $i \neq j$. It is clear that in (10), all blocks except those involving E_{ij}'s and E_{ji}'s will become zero matrices, resulting in a cross-shaped $\mathrm{d}S$ matrix (non-zero blocks in j-th block row and j-th block column only). Furthermore, for any 2-by-2 matrix A,

$$\operatorname{tr}(A\ \mathrm{d}E_{ij}) = \frac{\left\langle \mathrm{d}\mathbf{p}_j, (I-E_{ij})(A+A^\top)(\mathbf{p}_j-\mathbf{p}_i)\right\rangle}{\|\mathbf{p}_j-\mathbf{p}_i\|^2}.$$

From the above results, (9) considered as a partial derivative with respect to $\mathbf{p}_j$ can be written as

$$-\operatorname{tr}(S^\dagger S^\dagger \mathrm{d}S)\big|_{\mathrm{d}\mathbf{p}_i=\mathbf{0}, i\neq j} = \langle \mathrm{d}\mathbf{p}_j, \mathbf{c}_j\rangle,$$

where $\mathbf{c}_j$ is defined by

$$\mathbf{c}_j \triangleq -2\sum_{i,i\neq j} \frac{k_{ij}(I-E_{ij})(X_{jj}-X_{ij}-X_{ji})(\mathbf{p}_j-\mathbf{p}_i)}{\|\mathbf{p}_j-\mathbf{p}_i\|^2}.$$

If we compute $\mathbf{c}_j$ for all $j \in \mathcal{I}$, the stacked vector

$$\mathbf{c} = \begin{bmatrix} \mathbf{c}_1^\top & \mathbf{c}_2^\top & \cdots & \mathbf{c}_n^\top \end{bmatrix}^\top$$

is actually the gradient of the objective function with respect to variations in $\mathbf{p}$. The steepest descent direction of the cost function in (8) is then given by $-\frac{\mathbf{c}}{\|\mathbf{c}\|}$.

With the knowledge of the gradient of objective function, many well known optimization methods that require only first-order derivative information, such as the gradient methods and the quasi-Newton methods [13], can be used to find an approximate optimal solution to problem (7).

V. Topology Optimization

In this section, we look for methods that can increase the rigidity index of a KP-formation by changing K (i.e., formation topology) for fixed agent positions $\mathbf{p}$, subject to the connectivity constraint that the number of edges needs to be kept constant. The worst-case rigidity index r_{w} is used as the rigidity index to be maximized in the objective function. The reason for this choice is that, compared with MRI in the previous section, the variations in WRI under changing formation topology are easier to characterize. In addition, as remarked after problem (7) in Section III, the two indices tend to favor similar KP-formations.

A. Rank-One Update

Suppose that we start from an initial formation with agent positions $\mathbf{p}$ and connectivity matrix K. We assume that the initial formation with a stiffness matrix S is rigid, for otherwise the rigidity index may remain zero even after changing the topology. In this section, the secular equation ([14]) and a bisection algorithm proposed in [15] will be used for finding the optimal formation topology K.

When a single edge is added to or removed from the formation graph, the original stiffness matrix S is updated by a rank-one modification. Specifically, suppose an edge between nodes i and j with positions $\mathbf{p}_i$ and $\mathbf{p}_j$ is added (or removed). Define $\mathbf{e}_{ij} = (\mathbf{p}_j - \mathbf{p}_i)/\|\mathbf{p}_j - \mathbf{p}_i\| \in \mathbb{R}^2$. Then the stiffness matrix $\tilde{S}$ of the new formation is given by

$$\tilde{S} = S + \rho \Delta S.$$

Here $\Delta S = k_{ij}\mathbf{z}\mathbf{z}^\top$, where $\rho = 1$ (or -1) if the edge is being added (or removed), and $\mathbf{z} = [\mathbf{z}_1^\top \quad \cdots \quad \mathbf{z}_n^\top]^\top$ is a stacked vector in $\mathbb{R}^{2n}$ whose blocks $\mathbf{z}_k \in \mathbb{R}^2$ are defined by

$$\mathbf{z}_k = \begin{cases} \mathbf{e}_{ij} & \text{if } k = i \\ -\mathbf{e}_{ij} & \text{if } k = j \\ 0 & \text{otherwise.} \end{cases}$$

The strategy we propose here to maximize WRI is to add an edge that leads to the greatest increment to WRI, and then delete an edge with the smallest decrement. Thus each execution of this process involves two rank-one updates to the stiffness matrix. The following general theorem can be used to characterize how the spectrum of the stiffness matrix is affected by this rank-one modification.

Theorem 1 ([14]): Let $C = D + \sigma \mathbf{b}\mathbf{b}^\top$, where $C \in \mathbb{R}^{2n\times 2n}$ is a symmetric matrix; $D = \mathrm{diag}(d_1, d_2, \ldots, d_{2n}) \in \mathbb{R}^{2n\times 2n}$ is diagonal; $\mathbf{b} \in \mathbb{R}^{2n}$ and $\sigma \in \mathbb{R}$. Suppose $\bar{d}_1 \le \bar{d}_2 \le \cdots \le \bar{d}_{2n}$ are the eigenvalues of C. Then,

$$\begin{aligned} &d_1 \le \bar{d}_1 \le d_2 \le \bar{d}_2 \le \cdots \le d_{2n} \le \bar{d}_{2n}, \quad \text{if } \sigma > 0 \\ &\bar{d}_1 \le d_1 \le \bar{d}_2 \le d_2 \le \cdots \le \bar{d}_{2n} \le d_{2n}, \quad \text{if } \sigma < 0. \end{aligned}$$

As a result of the above theorem, if an edge is added, then $\lambda_4(\tilde{S})$ is between $\lambda_4(S)$ and $\lambda_5(S)$. On the other hand, if an edge is deleted, then $\lambda_4(\tilde{S})$ is between 0 and $\lambda_4(S)$. Furthermore, it has been shown in [14] that any eigenvalue of the modified stiffness matrix $\tilde{S}$ must be a root of the *secular equation* defined as below,

$$\begin{aligned} \omega(\mu) &\triangleq 1 + \rho k_{ij} \bar{\mathbf{z}}^\top (D - \mu I)^{-1} \bar{\mathbf{z}} \\ &= 1 + \rho k_{ij} \sum_{k=1}^{2n} \frac{\xi_k^2}{\lambda_i - \mu}, \end{aligned} \tag{11}$$

where $QDQ^\top$ is the diagonalization of S, $\bar{\mathbf{z}} = Q^\top \mathbf{z}$ and $\xi_1, \xi_2, \ldots, \xi_{2n}$ are components of $\bar{\mathbf{z}}$. The secular equation as a scalar equation can be easily solved numerically to yield all the eigenvalues of the modified stiffness matrix $\tilde{S}$.

B. Fast Rigidity Computation by Eigenvalue Update

As discussed in the previous section, when a single edge is added to the original formation graph, the WRI of the new formation graph will lie between the forth and the fifth smallest eigenvalues of the stiffness matrix of the original graph. Table I illustrates an algorithm called the *Edge Addition Bisection Algorithm* that can be used to determine which additional edge to add for maximizing the WRI.

TABLE I
Edge Addition Bisection Algorithm

Input	$\rho = 1$, $l = \lambda_4(S)$, $u = \lambda_5(S)$, $m = (l+u)/2$, $\mathcal{A}_0 = \mathcal{E}^{\complement}$ and $t = 0$
Step 1	If $\lvert\mathcal{A}_t\rvert = 1$, then go to Output; otherwise, $\mathcal{A}^+ = \phi$, $\mathcal{A}^- = \phi$, and go to **Step 2**.
Step 2	For each $e_{ij} \in \mathcal{A}_t$, if $\omega_{ij}(m) > 0$, then $\mathcal{A}^- \leftarrow \mathcal{A}^- \cup \{e_{ij}\}$; Otherwise, $\mathcal{A}^+ \leftarrow \mathcal{A}^+ \cup \{e_{ij}\}$
Step 3	If $\lvert\mathcal{A}^+\rvert = 0$, $u \leftarrow m$ and $\mathcal{A}_{t+1} = \mathcal{A}^-$ otherwise, $l \leftarrow m$ and $\mathcal{A}_{t+1} = \mathcal{A}^+$
Step 4	$t \leftarrow t+1$ and go to **Step 1**
Output	$\mathcal{A}_t$ (singleton)

Suppose one edge $\hat{e}_{ij} \in \mathcal{E}^{\complement}$ is added to G to form $G' = (\mathcal{V}, \mathcal{E}')$ where $\mathcal{E}' = \mathcal{E} \cup \hat{e}_{ij}$. Note that the new WRI is a solution of the secular equation (11) in the open interval $(\lambda_4(S), \lambda_5(S))$, and $\omega(\mu)$ is non-decreasing on this interval. Thus, the bisection algorithm can be used to find the best edge with the largest WRI.

Instead of applying the bisection algorithm to find the WRI for every possible edge $\hat{e}_{ij} \in \mathcal{E}^{\complement}$ to be added, we propose a more efficient algorithm called the *Edge Addition Bisection Algorithm* that performs the bisection operation for the secular equations associated with all these edges *simultaneously* to find the one resulting in the largest WRI. Suppose l and u are the current lower and upper bounds of

TABLE II

EDGE SWITCHING ALGORITHM

Input	Connectivity matrix K;
Step 1	Run Edge Addition Bisection Algorithm, then update K by adding the returned edge e_{add};
Step 2	Run Edge Removal Bisection Algorithm, then update K by deleting the returned edge e_{delete};
Step 3	If $e_{\text{add}} = e_{\text{delete}}$, then go to **Output**; otherwise go to **Step 1**
Output	K.

the WRI for the stiffness matrix of the current edge set $\mathcal{A}_t$ (with initial feasible edge set $\mathcal{A}_t = \mathcal{E}^{\complement}$ at $t = 0$), and let $m = (l + u)/2$ be the mid point. Then, the following rules

$$(i) \quad \omega(m) < 0 \;\Rightarrow\; r_{\text{w}}(\tilde{S}) \in [m, u]$$
$$(ii) \quad \omega(m) > 0 \;\Rightarrow\; r_{\text{w}}(\tilde{S}) \in [l, m]$$

can be used to divide the set of edges in $\mathcal{A}_t$ into two subsets: $\mathcal{A}^- = \{e_{ij} \in \mathcal{A}_t | \lambda_4(\tilde{S}) \in [l, m)\}$ and $\mathcal{A}^+ = \{e_{ij} \in \mathcal{A}_t | \lambda_4(\tilde{S}) \in [m, u]\}$. If the subset $\mathcal{A}^+$ is empty (i.e., $\mathcal{A}^-$ contains all candidate edges), then the midpoint m becomes the new upper bound and the new feasible edge set $\mathcal{A}_{t+1}$ is updated to $\mathcal{A}^-$; otherwise m becomes the new lower bound and $\mathcal{A}_{t+1}$ is updated to $\mathcal{A}^+$. This process is repeated until only one edge is left in the current feasible set $\mathcal{A}_t$.

The above idea can also be applied to the similar problem of deleting one edge while still maintaining the largest WRI. In this case, the new WRI lies inside the interval $(\lambda_3(S) = 0, \lambda_4(S))$; and since $\rho = -1$, $\omega(\mu)$ in the secular equation (11) is non-increasing on this interval. Correspondingly, the following changes to the Edge Addition Bisection Algorithm must be made to obtain the *Edge Removal Bisection Algorithm*: $\rho = -1$, $l = \lambda_3(S)$, $u = \lambda_4(S)$ and $\mathcal{A}_t = \mathcal{E}$ in the **Input**; in the **Step 2**, if $\omega(m) < 0$, then $\mathcal{A}^+ \leftarrow \mathcal{A}^+ \cup e_{ij}$, otherwise $\mathcal{A}^- \leftarrow \mathcal{A}^- \cup e_{ij}$.

C. Edge Switching Algorithm

By cascading the two bisection algorithms, we obtain a combined algorithm that maximizes the WRI by first adding and then deleting an edge from the formation graph. When the edges being added and deleted are not the same, the net effect is to relocate an edge within the formation graph. Table II illustrates the resulting *Edge Switching Algorithm*.

Fig. 1 shows a step-by-step illustration of applying the Edge Switching Algorithm to a simple example. The worst-case rigidity index of the example in Fig. 1 increases from 0.268 to 0.586 due to the topology optimization.

VI. ALTERNATING POSITION AND TOPOLOGY OPTIMIZATIONS

Based on the optimization algorithms introduced in Sections IV and V, we propose an *alternating method* for formation rigidity optimization, which is illustrated in Table III. The idea of the algorithm is to alternatively apply the position optimization and topology optimization processes until both fail to improve the formation rigidity any further.

TABLE III

ALTERNATING OPTIMIZATION ALGORITHM

Input	Original KP-formation $(\mathcal{I}, K^{(0)}, \mathbf{p}^{(0)}), t = 0$
Step 1	Fix $K^{(t)}$, optimize $\mathbf{p}^{(t+1)} = \arg\max_{\mathbf{p}} \bar{r}(S(K^{(t)}, \mathbf{p}))$ locally from $\mathbf{p}^{(t)}$ (Section IV)
Step 2	Fix $\mathbf{p}^{(t+1)}$, optimize $K^{(t+1)} = \arg\max_{K} r_{\text{w}}(S(K, \mathbf{p}^{(t+1)}))$ locally from $K^{(t)}$ (Section V)
Step 3	If $\bar{r}(S(K^{(t+1)}, \mathbf{p}^{(t)})) < \bar{r}(S(K^{(t)}, \mathbf{p}^{(t)}))$ or $\bar{r}(S(K^{(t+1)}, \mathbf{p}^{(t+1)})) = \bar{r}(S(K^{(t)}, \mathbf{p}^{(t)}))$, go to **Output**
Step 4	$t := t + 1$, go to **Step 1**
Output	$K^{(t)}, \mathbf{p}^{(t)}$

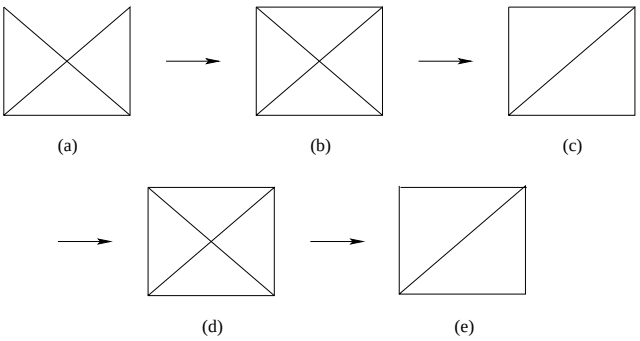

Fig. 1. Edge Switching Algorithm (a) **Input** → (b) **Step 1** → (c) **Step 2, Step 3** → (d) **Step 1** → (e) **Step 2, Step 3** then **Output**

Since we have used different objective functions in the two optimization problems, verification of consistency between the two objective functions becomes necessary when we merge the two optimization processes in Sections IV and V into one. This verification is done through the first condition described in **Step 3** of the algorithm in Table III.

An important advantage of the alternating method is that it can avoid some local extrema with poor overall value. The reason is that an extremum in agent positions may not be an extremum in topology, and vice versa. By switching between two objective functions, the optimal value obtained can be improved compared to non-alternating algorithm.

VII. EXAMPLE

Fig. 2 depicts the simulation results of the alternating formation optimization algorithm for a five-agent system under the connectivity constraint. The initial formation has random agent positions and a given topology as shown in Fig. 2(a). We first keep the topology unchanged, and apply the gradient descent algorithm to update the agent positions. The resulting local maximum of the MRI is shown in Fig. 2(b). The initial and final positions are shown by hollow and solid dots, respectively, and the dashed lines represent the trajectories of the intermediate results during

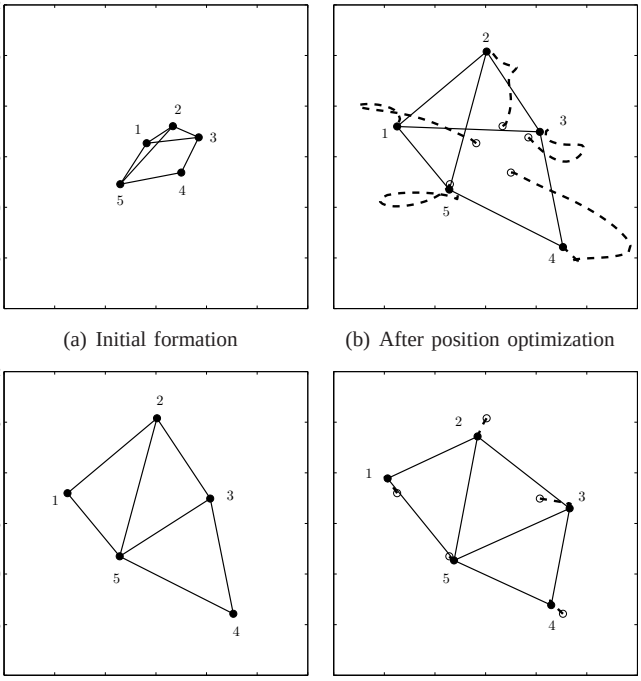

(a) Initial formation (b) After position optimization

(c) After topology optimization (d) Final formation

Fig. 2. Example on Alternating Optimization Algorithm

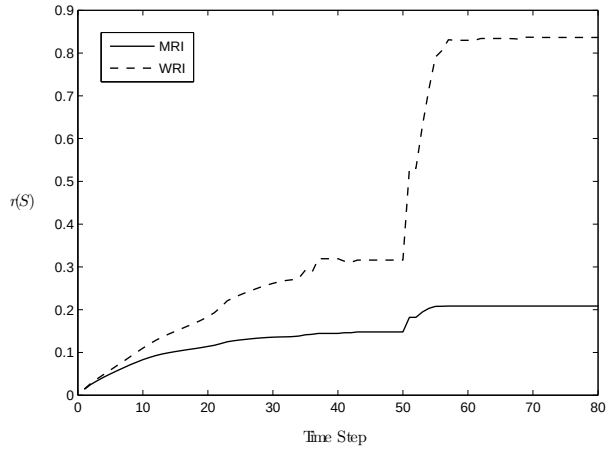

Fig. 3. Rigidity Indices versus Time step

the agent position optimization process. After the formation is locally optimized with the given topology, the edge-by-edge switching algorithm is applied to find the optimal topology for the new agent locations. The result is shown in Fig. 2(c). These two steps are repeated alternatively until neither of them can lead to an improvement. The final optimized configuration is rendered in Fig. 2(d).

Fig. 3 plots the rigidity indices: WRI and MRI, as functions of the time steps for the example in Fig. 2. Both rigidity indices increase during the execution of the formation optimization algorithm. The MRI grows from 0.0137 to 0.2084, while the WRI grows from 0.0145 to 0.8365. There exists a sudden improvement of the MRI from 0.1478 to 0.1820 (from 0.3160 to 0.5302 for the MRI) at time step 50 when topology optimization occurs. As can be seen from the figure, the MRI exhibits a similar general trend but with a smoother variation compared with the WRI.

VIII. Conclusion

Formation optimization is an important problem in multi-agent systems, such as sensor networks and UAV's. In this paper, we try to optimize the rigidity of a given formation as measured by two rigidity indices by reconfiguring the positions and the connection topology of the agents while conserving the total number of connections. We propose a solution to this constrained optimization problem by breaking it up into two phases: agent positions optimization and topology optimization. An alternating algorithm is proposed, whose effectiveness is demonstrated by examples. A future direction is to find a distributed version of this algorithm.

References

[1] B. Anderson, C. Yu, B. Fidan, and D. Van der Walle, "UAV formation control: theory and application," *Recent Advances in Learning and Control*, pp. 15–34, 2008.

[2] P. Bhatta, E. Fiorelli, F. Lekien, N. E. Leonard, D. A. Paley, F. Zhang, R. Bachmayer, R. E. Davis, D. M. Fratantoni, and R. Sepulchre, "Coordination of an underwater glider fleet for adaptive sampling," in *Proc. International Workshop on Underwater Robotics*, Genoa, Italy, 2005, pp. 61–69.

[3] R. Olfati-Saber and R. Murray, "Graph rigidity and distributed formation stabilization of multi-vehicle systems," *Proc. 41st IEEE Conf. Decision and Control*, vol. 3, pp. 2965–2971, Dec. 2002.

[4] B. Fidan, C. Yu, and B. Anderson, "Acquiring and maintaining persistence of autonomous multi-vehicle formations," *IET Control Theory and Applications*, vol. 1, no. 2, pp. 452–460, 2007.

[5] R. Olfati-Saber and R. Murray, "Distributed cooperative control of multiple vehicle formations using structural potential functions," in *Proc. 15th IFAC World Congress*, Barcelona, Spain, 2002, pp. 1–7.

[6] G. Laman, "On graphs and rigidity of plane skeletal structures," *Journal of Engineering mathematics*, vol. 4, no. 4, pp. 331–340, 1970.

[7] T. Tay and W. Whiteley, "Generating isostatic frameworks," *Structural Topology*, vol. 11, pp. 21–69, 1985.

[8] W. Whiteley, "Some matroids from discrete applied geometry," in *Proc. Ams-IMS-Siam Joint Summer Research Conference on Matroid Theory*, vol. 197. University of Washington, Seattle: American Mathematical Society, Jul. 1995, pp. 171–311.

[9] T. Eren, B. Anderson, A. Morse, W. Whiteley, and P. Belhumeur, "Information structures to control formation splitting and merging," in *Proc. American Control Conf., Boston, MA*, 2004, pp. 4951–4956.

[10] G. Zhu and J. Hu, "Stiffness matrix and quantitative measure of formation rigidity," in *Proc. 48th IEEE Conf. Decision and Control & 28th Chinese Control Conf.*, Dec. 2009, pp. 3057–3062.

[11] C. Chang and A. Sahai, "Estimation bounds for localization," in *IEEE SECON*, 2004, pp. 415–424.

[12] J. Magnus and H. Neudecker, *Matrix differential calculus with applications in statistics and econometrics. Revised ed.* John Wiley, Chichester, 1999.

[13] E. Chong and S. Żak, *An introduction to optimization.* Wiley-Interscience, NJ, 2008.

[14] J. Bunch, C. Nielsen, and D. Sorensen, "Rank one modification of the symmetric eigenproblem," *Numer. Math.*, vol. 31, no. 1, pp. 31–48, 1978.

[15] Y. Kim, "Bisection algorithm of increasing algebraic connectivity by adding an edge," *IEEE Trans. Autom. Control*, vol. 55, no. 1, pp. 170–174, Jan 2010.